Assessing Stability in Renewable Microgrid Using a Novel-Optimized Controller for PVBattery Based Micro Grid with Opal-RT Based Real-Time Validation

Anshuman Satpathy , Naeem M.S. Hannon , Rahimi Baharom * , Niranjan Nayak , Snehamoy Dhar

Posted Date: 16 July 2024

doi: 10.20944/preprints202407.1311.v1

Keywords: solar PV; duty-cycle; feedback controller; voltage control; IDGC; ELM; irradiance variation; partial shading

Article

Assessing Stability in Renewable Microgrid Using a Novel-Optimized Controller for PVBattery Based Micro Grid with Opal-RT Based Real-Time Validation

Anshuman Satpathy [1], IR Rahimi Bin Baharom [2,*], Naeem M. S. Hannon [2], Niranjan Nayak [3] and Snehamoy Dhar [3]

[1] Department of EE, Siksha 'O' Anusandhan Deemed to Be University, Bhubaneswar 751030, India; anshumanas1001@gmail.com
[2] School of Electrical Engineering, College of Engineering, Universiti Technologi MARA, 40450 Shah Alam, Malaysia , rahimi6579@uitm.edu.my, naeem@uitm.edu.my
[3] Department of EEE, Siksha 'O' Anusandhan Deemed to Be University, Bhubaneswar 751030, India; niranjannayak@soa.ac.in, snehamoydhar@soa.ac.in
* Correspondence: rahimi6579@uitm.edu.my

Abstract: This paper focuses on distributed generation (DG) controller of a PV based Micro Grid. An independent DG controller (IDGC) is designed for PV applications to improve maximum power point tracking (MPPT) in Micro Grid (MG). Extreme learning machine (ELM) based MPPT method exactly estimate the reference input of converter control. They are voltage and current at MPP. Feedback controls employ linear PI schemes or nonlinear, intricate techniques. Here the converter controller, IDGC is improved by measuring directly converter outputs like duty cycle. PWM index in a single DG PV based MG. It introduces a fast-learning Extreme Learning Machine (ELM) using Moore-Penrose pseudo-inverse and an online-sequential ridge re method for robust CR estimation. The approach ensures stability of the Micro Grid during PV uncertainties. Internal DG control approach (IDGC) improves the stability of the Micro Grid during, three phase fault at load bus, partial shading, irradiance change, islanding operation and load change. The model is designed and simulated in MATLAB/SIMULINK platform and some of the results are validated in hardware in simulation (HIL) platform.

Keywords: solar PV; duty-cycle; feedback controller; voltage control; IDGC; ELM; irradiance variation; partial shading

1. Introduction

In the current energy market, the focus on limiting environmental pollution, particularly greenhouse gases, has prompted the need for modern design standards in conventional power systems. Depletion of fossil fuel reserves and notable power losses have increased the reliance on Renewable Energy Sources (RESs), including PV and Wind Generation S (WG), in traditional grid frameworks[1,2]. The MG operations primarily focus on integrating local loads in the distribution network to enhance Power Quality and system reliability. Distributed Generations (DGs) encompass converter stations and associated components, ensuring stable and reliable power dispatch. DGs serve as alternatives to traditional electricity generation methods, offering a range of scientific options from RE & non RE sources. These systems can operate in on-grid or off grid modes, providing flexibility and resilience to the power infrastructure. Renewable energy-based DGs effectively alleviate power crises in central grid buses. Leveraging various sources such as solar photovoltaic, wind generation, fuel cells and (CHP) systems, biofuels, and micro-turbines, DGs offer advantages

 doi:10.20944/preprints202407.1311.v1

for small-scale localized grids. These include reduced carbon emissions, long-term asset viability, dynamic power regulation, and suitability for rural applications, making them invaluable contributors to sustainable energy solutions. The countries like India where there are abundant sunlight is available, is suitable for solar production. Now India has become stronger in solar power generation and PV infra-structure.

PV-based DGs are extensively documented in literature [4–6], conforming to IEEE 1547 standards, requiring capability for both grid interactive and islanded modes [4]. As suggested in [5,6], the control Hierarchical structures for effective management of PV-based DG systems. ISA-95 standards endorse hierarchical structures for distribution-level PV DG solutions, such as Rooftop PV installations, facilitating coordinated distributed control. By this application PV operates at maximum power points with MPPT algorithm [7–10]. The conventional MPPT control algorithm like P&O. INC and Hill climbing are best suitable in simplicity and low operational cost. However they are not good performer in partial shading conditions [7]. Other methods like Fuzzy based MPPT needs pre requisite information and have high computational burden [8]. On the other hand artificial neural network (ANN) based MPPT has high speed computation and well performed in shading condition [9].However, ANN's learning architecture, such as feedback bias, hinder its adoption in small-scale PV solutions. Following ISA-95 standards, the ordered controller comprises a Primary Controller (PC) and (IDGCs). In managing Distributed Generation (DG) systems, Control References (CRs) are crucial for effective energy management. To achieve this, Integrated Distribution Grid Controllers (IDGCs) function as closed-loop feedback controllers, overseeing Converter stations on the PV side. These IDGCs employ duty cycle calculation for PV-DC operation and (PWM) based (PLL) operations, ensuring coordination within distributed PV systems while adhering to standardized protocols. In PV-based DG applications, cost-effective solutions are paramount for managing local loads. Integration of Independent DG Controllers, encompassing (MPPT) tracking and feedback control for duty measurement, is vital for stability analysis. To tackle computational complexity, Artificial Neural Network (ANN) based control algorithms offer a promising avenue. Here, solar irradiation (W/m2) and PV panel temperature (°C) serve as control inputs, while duty reference for DC Voltage Boost operation is the output. This optimized approach, implemented every k_{th} iteration with a computational clock time constant (ΔT intervals), streamlines computational burden while enhancing accuracy in CRs calculation. Consequently, it ensures the efficient operation of PV-based DG systems, mitigating computational overheads, and maintaining stability.

As discussed in [17] a novel deep representation-based (MPPT) controller for precise Control references calculation in Photovoltaic (PV) based Micro Grid (MG) operation. The approach involves a two-step estimation process: Data dimension reduction and MPPT Tracker optimization for efficient computation. Targeted for a large number (N) of PV-based DGs locally connected in the distribution system, the method utilizes Extreme Learning Machine (ELM) for data dimension reduction and Ridge Regression-based ELM for MPPT error estimation at the Tertiary Control side.

The standard power recognizing controllers may localize the functioning point of PV rather than capturing the global working point as depicted in the literature. The conventional neural controller depicted in[9] requires substantial expertise in static analysis and calculus, along with extensive training and loading data. Neural designs consist of interconnected neurons organized in multiple layers, with biological neurons represented as nodes. Data processing occurs from the input layer to the output. Similarly, multilayer power point finding controllers incorporate multiple hidden layers, leading to increased implementation complexity and high computational time.

In [18–22], authors propose a soft computing approach using fuzzy logic to track MPP variations in solar PV systems. They introduce a variable step radial basis functional controller fused with fuzzy logic to improve upon conventional fuzzy controllers in partially shaded conditions. This hybrid controller combines the strengths of fuzzy logic and artificial neural networks (ANN) to optimize MPPT. While fuzzy logic and ANN methods are effective, they can be computationally burdensome. Integrating these methods offers a robust solution to nonlinear problems, enhancing MPPT efficiency in challenging conditions. To overcome the challenges from fuzzy and ANN based MPPT controller,

 doi:10.20944/preprints202407.1311.v1

This paper introduces a streamlined approach using a single-layer, feed-forward (ELM) to enhance computation time efficiency.

Here the online sequential learning method with Ridge Regression Regularization, is applied to optimize the training output weights for ELM-IDGC. Motivation and problem formulation and literature survey are discussed in section-1. Section-2 describes the architecture of PV based micro grid with detailed specifications. This section also covers boost operation with linear PI control based duty measurement. The ELM-based IDGC operation is outlined in section 3, emphasizing online training methods. Section 4 validates the performance of this control approach, presenting MATLAB-based results that demonstrate improved stability with the proposed ELM-IDGC. Finally, section 5 offers an overall discussion and summary of the research findings.

2. Considered PV Based DG

Photo voltaic a popular RES, employs cells or modules arranged in series and parallel to form arrays tailored to load needs. These arrays, integrated into local distribution networks as DGs, utilize DC-DC and/or DC-AC converters. This section models PV-based DG, integrating converter dynamics for feedback control.

The PV system under consideration is rated at 140 kW with a voltage of 17 volts at standard test conditions (STC: 1000 W/m2, 25°C). Prior to grid power dispatch, it is integrated with a DC-DC converter station (Figure 1). This study focuses on DC Voltage Boost u_{bo} operation to maintain a consistent DC bus voltage profile u_{dck}, where 'k' represents the control operation instant. The primary objective is to assess (CR) error and its impact on DG stability. Therefore, a voltage feedback control, or (IDGC), is devised to estimate duty cycles for DC u_{bo} operation.

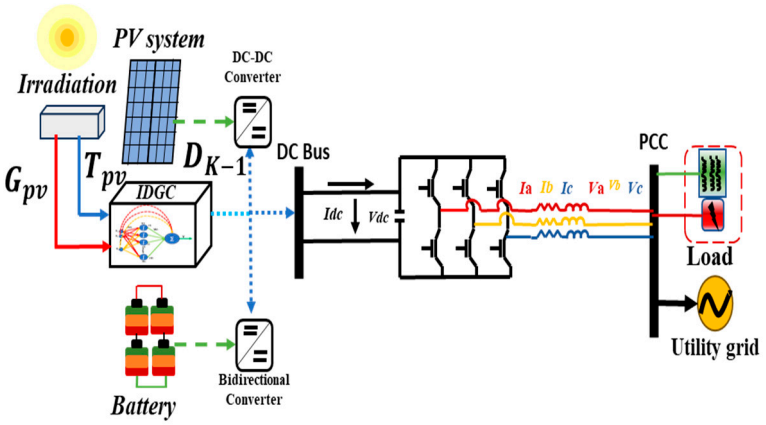

Figure 1. Considered PV based Micro Grid.

2.1. Modelling with Conventional MPPT

Here a proto type real world PV module (140 watt, 17 volt) are designed with single diode and standard specifications [5]. The circuit contains series & parallel resistances. For generalized PV cells, initial voltage drop and internal resistance ir are considered. From Kirchhoff's Current Law (KCL) in the PV circuit, Eq. (1) derives the cell's output current.

$$i = i_{ph} - i_{rst}\left[\exp\left(\frac{u + ir_s}{au_T}\right) - 1\right] - \left(\frac{u + ir_s}{r_{sh}}\right) \tag{1}$$

For a common PV cell, r_s and r_{sh} range from 0.02 to 0.13 Ω and 210 to 487 Ω, respectively. i_{ph} is determined as:

$$i_{ph} = 0.01 \times G_{PV} \times [i_{sc} + k_i(\Gamma_{PV}^{*} - \Gamma_{PV})] \tag{2}$$

 doi:10.20944/preprints202407.1311.v1

G_{PV} Signifies solar irradiation (W/m2), k_i is the short-circuit current temperature coefficient, attainable from data sheet. Γ^*_{PV} and Γ_{PV} indicate temperatures at STC and cell's operational temperature, respectively. The back saturation current i_{rst} is stated as:

$$i_{rst} = i_{rr}\left(\frac{\Gamma_{PV}}{\Gamma^*_{PV}}\right)^2 \times \exp\left[\frac{q \times E_g}{k \times a}\left(\frac{1}{\Gamma_{PV}} - \frac{1}{\Gamma^*_{PV}}\right)\right] \tag{3}$$

PV cells are arranged in series and parallel to form PV modules, which are then connected similarly to achieve desired power and voltage ratings. The PV system configuration, considering the number of series connected cells n_{se} and parallel connected cells n_{pp}, is expressed as:

$$i^k_{PV} = n_{pp} i^k_{ph} - n_{pp} i^k_{rst}\left[\exp\left(\frac{1}{u_T a} \times \left(\frac{u^k_{PV} + i^{k-1}_{PV} r_s}{n_{se}}\right)\right) - 1\right] - \left(\frac{\left(n_{se}/n_{pp}\right) u^k_{PV} + i^{k-1}_{PV} r_S}{r_{sh}}\right) \tag{4}$$

This section presents manufacturer details for a single 140 W PV module. The PV module is formed by connecting 3 modules in series, each rated at 3485.7 W and 317 volts. Additionally, 13 shunt strings are created, with 2 modules in series per string. The PV output features, such as u_{PVk} (Voltage) vs. P_{PVk} (Power) or u_{PVk} (Voltage) vs. i_{PVk} (Current), exhibit nonlinear behavior. To maximize power p_{MPP_k}, the DC u_{bo} voltage input should match the voltage at P_{MPP_k}, u_{MPP} depicted in Figure 1.The specifications of WS-140 PV panel as $p_{\max} = 140\ watt$, $u_{MPP} = 18 volt$, $i_{MPP} = 7.85\, amp$, open circuit voltage=22volt, SC current=8.95 Amp. Current temp coefficient=(0.065 ± 0.015)%/ ◦C.

That for voltage is -(80 ± 10)mV/ ◦C , NOCT= (47 ± 2) ◦C.

PV systems employing DC operation necessitate MPPT algorithms to ascertain u_{mppk}. Traditional linear MPPT methods (like P&O, Hill Climbing) offer iterative, exact findings but may inaccurately track under multiple p_{mppk} , such as partial shading conditions. Partial shading occurs when certain PV modules are unable to receive full exposure, impacting overall system efficiency. Non-linear MPPT methods, like Fuzzy logic [13] and (ANN) approaches [14], are well-documented. However, they impose computational burdens on PV-DG applications. Hence, this paper aims to enhance conventional iterative, back-propagation learning for a simpler solution.

2.2. Boost Converter Operation with Linear Feedback

The maximum power p_{mpp^k} and voltage at MPP u_{mpp^k} are the two inputs for designing the converter controller. The output of the converter is p_{dc^k} and u_{dc^k} are the converter power & voltage. The PV voltage and currents are expressed as

$$\dot{u}^{\mathrm{k}}_{\mathrm{dc}} = \frac{1}{u^{\mathrm{k}}_{\mathrm{dc}} C_{\mathrm{dc}}}\left[u^{\mathrm{k}}_{\mathrm{dc}} \sum_{n=1}^{N} i^{\mathrm{k}}_{\mathrm{dc},n}\left(1 - d^{\mathrm{k}}_{\mathrm{MPP}}\right) - p^{\mathrm{k}}_{\mathrm{dc}}\right] \tag{5}$$

 doi:10.20944/preprints202407.1311.v1

$$i_{\mathrm{dc},n}^{\mathrm{k}} = \frac{1}{L_{\mathrm{dc,n}}}\left(\frac{u_{MPP}^{\mathrm{k}}}{1-d_{MPP}^{\mathrm{k}}} - u_{\mathrm{dc}}^{\mathrm{k}}\right) \tag{6}$$

Here $n = 1, 2, \ldots N$, PV numbers, L_{dc} and C_{dc} are Converter inductance and capacitance. The d_{mpp^k} is k_{th} sampling instant for converter duty. The u_{bo} operation is guaranteed by feedback path, is given by equation (6).

$$d_{\mathrm{mpp}}^{\mathrm{k}} = d_{\mathrm{MPP}}^{\mathrm{k-1}} \pm \left[\begin{array}{l} \kappa_{\mathrm{P,dc}}\left(e_{\mathrm{dc}}^{\mathrm{k}}\right) \\ + \kappa_{\mathrm{I,dc}}\left(e_{\mathrm{dc}}^{\mathrm{k}} - e_{\mathrm{dc}}^{\mathrm{k-1}}\right) \times \Delta\Gamma_{\mathrm{s}} \end{array}\right] \tag{7}$$

Considered as control error, $e_{\mathrm{dc}}^{\mathrm{k}} = u_{\mathrm{dc}}^{*} - u_{\mathrm{mpp}}^{\mathrm{k}}$ a simple PI is implemented. $\Delta\Gamma_S$ is the sampling time. The considered duty cycle is then processed for IGBT switching in the DC Converter . Dynamic equations for the DC Converter are derived to design a stable output profile controller. A closed-loop feedback response is necessitated for the Feedback controller/(IDGC), adhering to ISA-95. Complying with IEEE 1547, to ensure both mode of operations of IDGC is prioritized for operational flexibility. Described here is the IDGC feedback path using a linear 2nd Order PI control.

3. Proposed DG Controller

The (IDGC), integrating MPPT and closed loop PI control for duty assessment, can benefit from a computationally efficient approach using Artificial Neural Network (ANN) based algorithms. Input parameters such as solar irradiation G_{PV} and PV panel heat Γ_{PV}, with output as duty reference for DC boost operation d_{mpp} streamline computations by directly converting G_{PV}, Γ_{PV} to d_{mpp}, omitting intermediate steps like u_{mpp}, p_{mpp} and e_{dc}. This reduction in calculations per iteration, enhances accuracy in calculating Control References (CRs).

To address the limitation of ANN-based IDGCs in real-time feasibility due to weight matrix estimation, a non-iterative Moore-Penrose Pseudo-inverse *MPPI* technique is employed for training. This technique, unlike conventional iterative methods, such as back-propagation, enhances efficiency and is applied to feed-forward ANN like (ELM) [9].

In Figure 3 (a), the traditional IDGC (following ISA-95 standard) involves two-step duty cycle designs, prone to Control Reference (CR) errors, potentially compromising DC bus stability. In Contrast, the proposed ELM-IDGC (Figure 3(b) streamlines computational steps and minimizes iterative learning, reducing computational delays. The fast, learning approach (MPPi) is advised for the ELM-IDGC, aiming to enhance stability. The linear relationship between duty cycle d_{mpp^k} and MPP voltage (VMPPk) depicted in Fig. 3 indicates predictable behavior. Variations in irradiation yield different u_{mpp^k} (Figure 3a) and d_{mpp^k} (Figure 3b). By leveraging linear functionality instead of non-linear nodes, the proposed IDGC anticipates improved stability. The ELM learning strategy is poised to swiftly and robustly reduce errors.

In ANN literature, numerous constructional and working enhancements are explored, ranging from basic feed-forward structures to complex architectures incorporating feedback bias. Operational methods span from traditional back-propagation and least square solutions to contemporary non-iterative (NI) techniques, enriching control algorithms' operational perspectives [9].

3.1. Redge Regression Based ELM

ELM has gained prominence as a feed-forward neural network (FFNN) in the past decade [23]. Because of its straightforward construction, different training techniques, such as least-square

Preprints.org (www.preprints.org) | NOT PEER-REVIEWED | Posted: 16 July 2024 doi:10.20944/preprints202407.1311.v1

solutions, are recommended for strong valuation of error reduction. In PV-based DG applications, literature predominantly focuses on either MPPT algorithms alone or feed-forward IDGC structures, where G_{PVk} and Γ_{PVk} are functions of d_{mppk} derived from linear MPPT data. However, adhering to ISA-95 and IEEE 1547 standards (Figure 2a), the entire operation, including traditional two-step MPPT tracing and closed-loop duty assessment, must be employed at the IDGC level. Hence, trained data for the proposed IDGC is acquired according to normal performs.

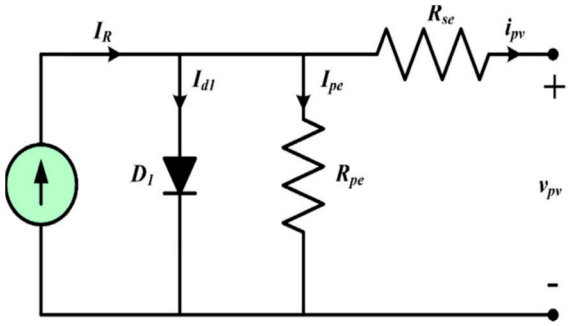

Figure 2. circuit diagram of a PV cell.

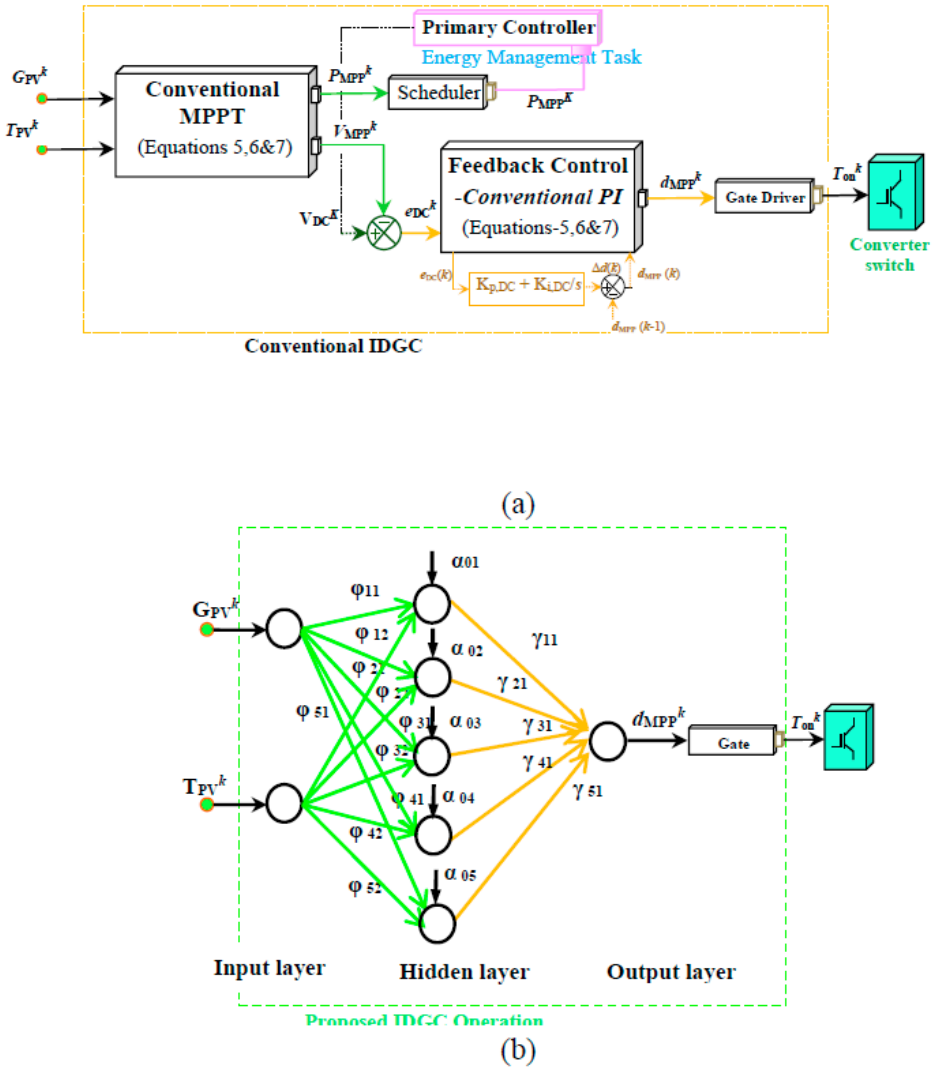

Figure 3. constructional diagram of PV-DG's IDGC with ISA-95 standard.

Preprints.org (www.preprints.org) | NOT PEER-REVIEWED | Posted: 16 July 2024 doi:10.20944/preprints202407.1311.v1

The structure of ELM comprises Input, Hidden, and Output Layers (i_L, h_L & o_L) respectively, to derive preferred probable Control References (CRs), such as d_{mppk} (Figure 2b). Table 2 presents common notations for clarity. The general ELM is single-layered, and training employs a , mpp_i inverse method [24]. IL nodes connect with arbitrary φ, while [γ] is derived from non-iterative training. In spite of arbitrariness, ELM can be designed with minimal e_{IDGCk} during training, outperforming conventional techniques. Unlike methods requiring both [φ] and [γ] from initial randomness in training, ELM exhibits improved generalized performance.

The Input layer node is given by

$$[\chi_{iL}]^k_{1\times A} = [\chi^k_{iL,1}, \chi^k_{iL,2}, \chi^k_{iL,2} \cdots\cdots \chi^k_{iL,A}] \tag{8}$$

And the output layer node is presented as

$$[\gamma_{oL}]^k_{1\times A} = [\gamma^k_{oL,1}, \gamma^k_{oL,2}, \gamma^k_{oL,2} \cdots\cdots \gamma^k_{oL,\mathbf{B}}] \tag{9}$$

Here *A* and *B* are input & output data size.

The hidden layer matrix is expressed as

$$[hL]^k_{1\times C} = [h^k_{L,1} \quad h^k_{L,2} \quad \ldots \quad h^k_{L,C}] = \begin{bmatrix} \sinh\left(\sum_{i=1}^{A}(\varphi^1_i \times \chi^k_{IL,1}) + \lambda_i\right) \\ \sinh\left(\sum_{i=1}^{A}(\varphi^2_i \times \chi^k_{IL,1}) + \lambda_i\right) \\ \vdots \\ \sinh\left(\sum_{i=1}^{A}(\varphi^C_i \times \chi^k_{IL,1}) + \lambda_i\right) \end{bmatrix}^T \tag{11}$$

Initially, $[\varphi]_{A\times C}$ is arbitrarily chosen from 0-1 during training. The sine hyperbolic activation function is employed for its adaptability to large e_{IDGCk} signatures. Post-training, estimated CR: d_{MPPk} is derived from the output layer node for real-time performance.

$$[E_{OL}]^k_{1\times B} = [h_L]^k_{1\times C} \times [\gamma]^k_{C\times B} \tag{12}$$

The *MPPI* is utilized for finalizing the $[\gamma]_{C\times B}$ with training data samples as:

$$[\gamma]^k_{C\times B} = \left[\left(hL^T \times hL\right)^{-1} hL^T + \frac{I}{R_C}\right]^k_{C\times 1} \times [\Gamma_{OL}]^k_{1\times B} \tag{13}$$

During supervised learning, the OL layer outputs for training samples, with a minimization formulation.

$$\min \zeta^k_\gamma = \frac{I}{2}\left\| \left[\left(hL^T \times hL\right)^{-1} hL^T\right]^k_{C\times 1} \times [\Gamma_{OL}]^k_{1\times B} - [E_{OL}]^k_{1\times B} \right\|^2 + \frac{r_C}{2}\left\| e^k_{IDGC} \right\|^2 \tag{14}$$

The Regularization coefficient is measured from [14].

$\varphi, h_L, \gamma, \alpha$ are the usual abreviations like input weights, hidden layer output matrix output weight, bias in output layer.

R_{c1}, e_{IDGC^k} are the regularisation and control reference error.

 doi:10.20944/preprints202407.1311.v1

3.2. Robust Estimation Enhanced via Online Learning, Refining Models Dynamically for Resilient Data Analysis and Accurate Parameter Estimation

Dynamic control enactment necessitates a state inform agenda to maintain balanced working conditions in PV DG applications. The ELM-based IDGC is trained via online sequential learning, where training data isn't entirely processed upfront. Instead, successive gaps (N data chunks) are treated iteratively, enhancing adaptability to changing conditions and facilitating real-time adjustments for improved performance.

$$[\gamma]_{C\times B}^{k+1} = [\gamma]_{C\times B}^{k} + \left(\left[\left(\mathrm{hL}^{T} \times \mathrm{hL} \right)^{-1} \mathrm{hL}^{T} + \frac{I}{r_C} \right]_{C\times l}^{k} \times [\Gamma_{OL}]_{l\times B}^{k} \right) - [E_{OL}]_{l\times B}^{k} \tag{15}$$

In connection with input layer node, $[\chi_{iL}]_{l\times A}^{k} = [G_{PV}, \Gamma_{PV}]_{l\times A/2}^{k}$ and output layer node $[\gamma_{OL}^{k}] = [d_{mpp}]_{l\times B}^{k}$ the ELMIDG is operated with PV-DG as shown in Figure 1. To improve the training performance of $[\gamma]_{C\times B}^{k+1}$ optimal with error e_{IDGC}^{k} reduction, the online sequential learning is applied.

4. Result Analysis

Here a single DG based Micro Grid is designed in MATLAB/SIMULINK platform. The model details are given in this section. The proposed ELM-IDGC controller has been applied to a 10 kw PV application. The model is simulated for 10, 40 60 seconds and the results are compared with the conventional method.

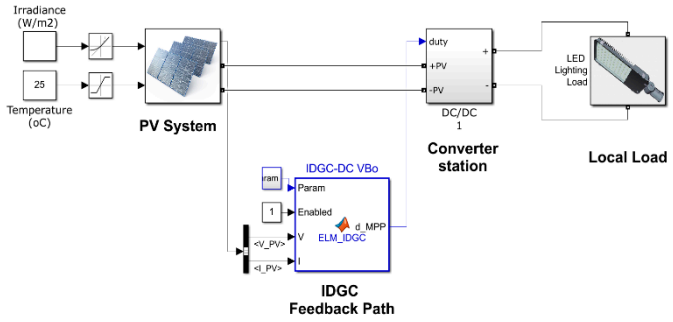

Figure 4. ELM-IDGC Simulink model.

The enactment is evaluated through various operating conditions like MPPT error minimization, Irradiance change, partial shading, islanding operation three phase fault and load change. The Micro Grid parameters are 12 kW, 100volt DC, dc link voltage 150 V (DC), 230 V, 50 Hz AC conversion and load rating is 10 kW, 0.784Ω LEDs. Converter to PCC impedance is 2km $0.1184 + j0.0042$ ohm.

Senario-1: MPPT Error minimization

During the operation the accuracy and computational burden are two major parameters to be measured. The efficacy of the proposed MPPT model is compared with the traditional linear & nonlinear techniques. Solar irradiance and the panel temperature are the two major input data to the MPPT. The RES data set is divided into different sets based on the seasons. During considered events like partial shading the seasonal data is resampled for RES-P_{PV} and V_{PV} estimation, with the uncertainty. The training and testing ratio of irradiance data is 7:3. Various performance matrices are described to estimate the MPPT error, which are formulated as following.

Preprints.org (www.preprints.org) | NOT PEER-REVIEWED | Posted: 16 July 2024 doi:10.20944/preprints202407.1311.v1

$$MAPE = \left[\frac{1}{N} \sum_{k=1}^{N} \frac{|P_k - \Gamma_k|}{P_k} \right] * 100$$

$$RMSE = \sqrt{\frac{1}{N} \sum_{k=1}^{N} |P_k - \Gamma_k|^2} \qquad (16)$$

$$MAE = \frac{1}{N} \sum_{k=1}^{N} |P_k - \Gamma_k|$$

Here total samples is 'N' and P_k and T_k are actual value and predictable value of the MPPT.

From the DAS data validation and the PCC of Micro Grid parameters, the performance of the proposed MPPT is judged. The DAS data with 5 minutes interval measures various error responses such as RMSE, MAPE. For long time interval the MPP will be erroneous for which 5 minutes interval is considered. Here the proposed ELM based IDGC has been implemented to estimate maximum power in a Micro Grid. Its performance is compared with basic MPPT controller. The entire PV data is classified into different seasons and here only summer data profile is validated. Figure 5 depicts RMSE 0.061% - 0.88% and MAPE 2.48%-4.48%. The RMSE of conventional & proposed are given in Pu 0.032-0.0038 respectivelly.The range of MAPEs in Pu are 0.0412-0.0622 and 0.1053-0.2348 conventional and proposed ELM respectively. It is evidently proved that proposed MPPT performs effectively better than the conventional MPPT.

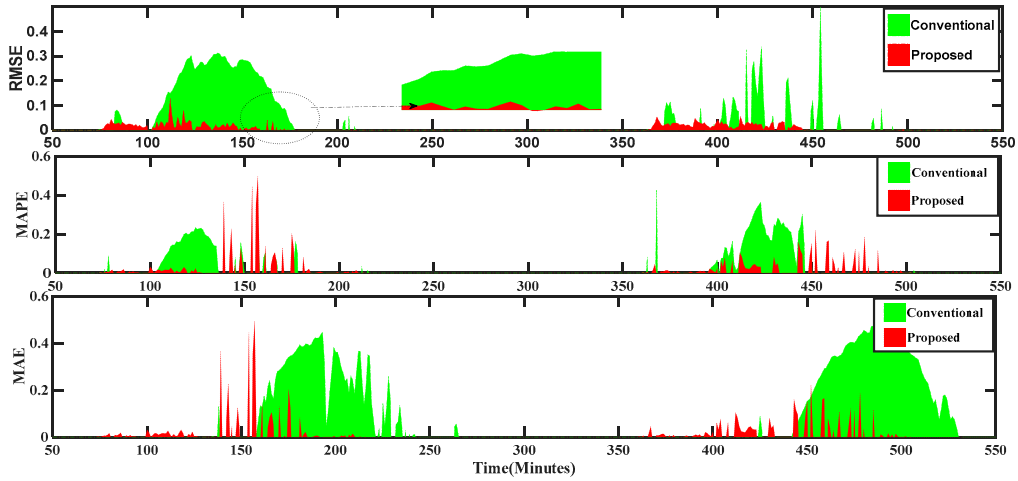

Figure 5. The original data set of MPPT.

Scenario-2: Performance under Irradiation Variation

The PV generated voltage and power is affected by the solar irradiance change, due to its intermittent nature. The irradiance depends upon the weather conditions. In sunny weather the substantial amount of irradiance is produced and the PV generates its rated power and voltage. But in rainy season and foggy weather the PV generation is affected. To compensate this challenge a battery energy storage (BES) is connected to the system. The intermittent nature of irradiance influence the DC link voltage and other parameter of MG also. The presentation of the proposed controller is investigated during irradiance variance through AC bus parameter disturbance. The fault clearance time is measured in seconds and cycles. The performances are listed in table-2. From the Figure 6, it is observed that the irradiance changed in three states. In each state the fault mitigates 1 second (50 cycles) but the conventional MPPT mitigates the fault in 10sec (200 cycles) in each state. The PV and IV charectestics of the PV cell is shown in Figure 6a,b respectively, during various states. The instability created in the MG is balanced by auxiliary power supply by the battery system given by the equation (17)

Preprints.org (www.preprints.org) | NOT PEER-REVIEWED | Posted: 16 July 2024 doi:10.20944/preprints202407.1311.v1

$$
\begin{aligned}
&if\ p_{pv} < p_{dcref} \\
&if\ 40 < soc < 80 \\
&p_{batt} = p_{dcref} - p_{pv}(discharging) \\
&else \\
&soc < 40 \\
&p_{batt} = 0 \\
&end \\
&else if\ \ p_{pv} > p_{dcref} \\
&if\ \ soc < 80 \\
&p_{batt} = -(p_{dc} - p_{pv})\ \ charging \\
&else\ \ soc > 80 \\
&p_{batt} = 0 \\
&end \\
&end
\end{aligned} \tag{16}
$$

Figure 6f,g, displays the battery voltage and current fluctuations amidst irradiance changes, showcasing the superior performance of the suggested IDGC over conventional methods. The Proposed method exhibits minimized power oscillation and transient variation during fault incidents. This confirms IDGC superiority in managing system dynamics, offering improved stability and efficiency compared to traditional techniques.

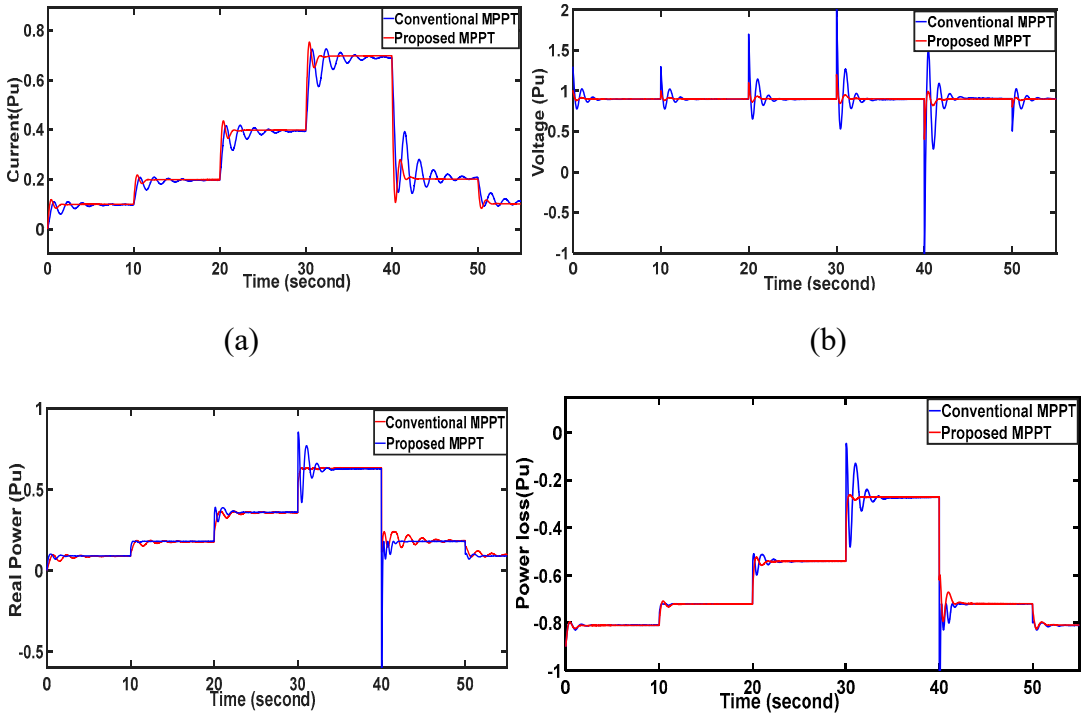

Preprints.org (www.preprints.org) | NOT PEER-REVIEWED | Posted: 16 July 2024 doi:10.20944/preprints202407.1311.v1

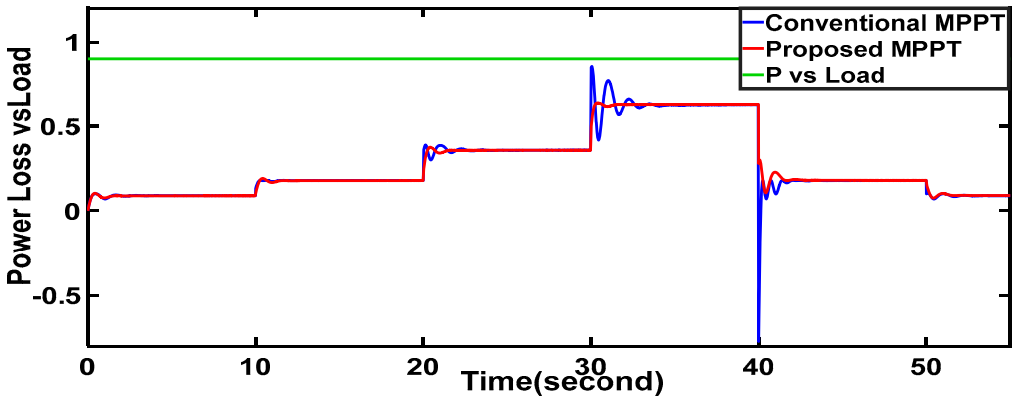

(e)

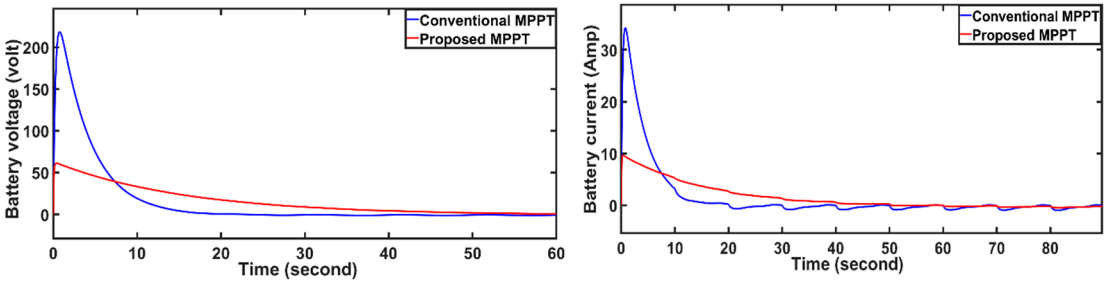

(f) (g)

Figure 6. Performance of IDGC controller in (a) DC current (b) DC voltage (c) Real Power (d) Power loss (e) Power loss verses load. (f) Battery voltage variation (g) battery current.

Table: comparisons of MPPT controller with 3 states.

MPPT Technique	State-1	State-2	State-3
Voltage ripple (V)			
Conventional	3.98	2.87	3.88
Proposed	0.08	0.04	0.03
Current ripple (A)			
conventional	0.93	0.49	0.054
Proposed	0.35	0.26	0.003
Convergence time (s)			
Conventional	0.051	0.042	0.045
proposed	0.0062	0.0084	0.003
Tracking Efficiency (%)			

 doi:10.20944/preprints202407.1311.v1

Conventional	96.98	96.92	97.10
Proposed	99.2	99.32	99.91
Overall efficiency			
Conventional	94.93	92.85	91.51
Proposed	97.93	97.83	97.81
RSME MPPT Error			
Conventional	0.00481	0.02471	0.03166
Proposed	0.00061	0.00181	0.00287
MAE Error			
Conventional	0.00561	0.02971	0.01861
Proposed	0.00049	0.00187	0.00297
MAPE Error			
Conventional	0.5289	2.831	4.105
Proposed	0.0812	0.198	0.536

Scenario-3: Partial shading

To achieve the rated power for a Multi-Panel Photovoltaic System (MPVS), the arrangement of PV panels in series and/or parallel configurations is crucial. Series connection boosts the output voltage, while parallel connection increases the PV array output current. Accurate modelling of the PV array, necessitates reproducing the actual current-voltage (I-V) characteristic curve of the PV cells. In literature, single and double diode models are commonly employed. The single diode model, simpler and less computationally intensive, is often favoured, particularly for demonstrating partial shading effects, offering satisfactory results with minimal complexity.

Under non-uniform irradiation, the power-voltage (P-V) characteristics of the PV array exhibit multiple peaks as shown in Figure 7a,b. The highest peak, termed the global maximum point (GM) and lowest is local maximum points (LM). The number of peaks correlates with the number of panels receiving varying power or irradiance levels, while the position of the GM depends on the intensity of irradiance and the arrangement of panels.

In this case a multi cell PV array is used as distributed generator of a MG. A 100 watt PV panel is taken with total 60 cells (connected 40 series and 20 parallel). As depicted in Figure 7, the partial shading is achieved by disconnecting individual cells. Here each cell is of 0.15volt and 1.5 watt. At t=5 sec, 2 cell (3 watts), at t= 10, two cells (3 watt) and at t= 40sec to 50 sec, 6 No of cells (0.9V, 9 watts) are disconnected. Further at t=80 sec two cells (0.3volt, 3 watt) are included. The disconnection of cells results the partial shading operation of PV module. The Cell reduction produces a disturbance in PV output and Micro Grid System. By this types of disturbance the DC voltage fluctuates by 2.5 Pu, approximately. Current fluctuated within 0.4 Pu. Similarly the deviation of real power, reactive power and active power loss by both MPPT controllers are shown in Figure 7. From the results it is confirmed that the proposed IDGC MPPT controller reduces the deviations quickly than the conventional controller.

Preprints.org (www.preprints.org) | NOT PEER-REVIEWED | Posted: 16 July 2024 doi:10.20944/preprints202407.1311.v1

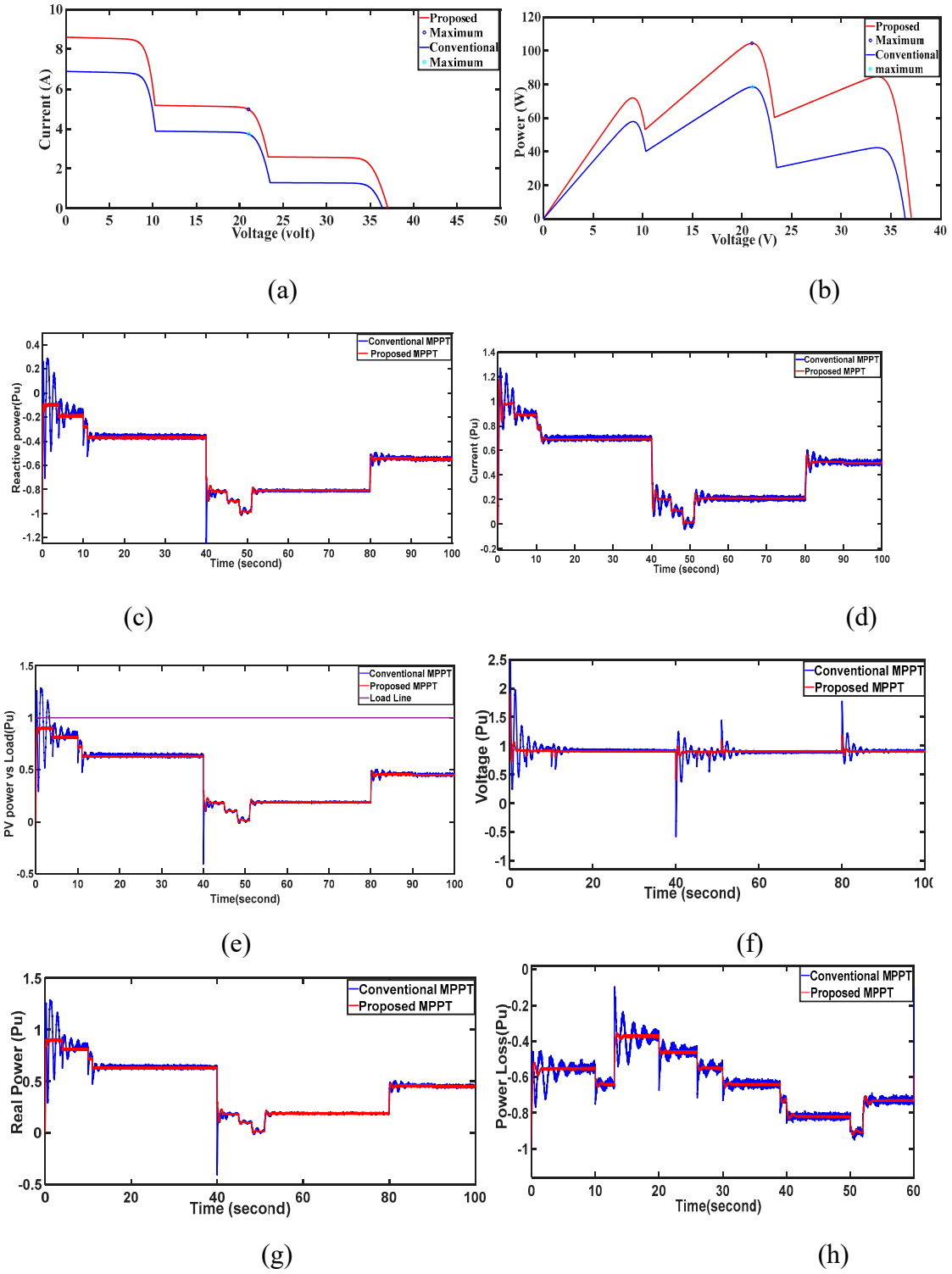

Figure 7. Performance Through Partial shading (a) I-V charecterstics (b)P-V charecterstics (c) Reactive power at AC bus (d) dc link current (e) PV power verses load (f) dc link voltage (g) real power (h) power loss.

Scenario -4: Three phase fault at Bus-1

The efficacy of the system with increased strength undergoes scrutiny in a three-phase fault scenario at bus-1 (PCC). Figure 8, illustrates the response of various grid and auxiliary power supply parameters. At t = 0.5 s, a five-cycle three-phase fault is introduced at the PCC. The IDGC technique swiftly damps oscillations, stabilizing the system within 2 seconds or 100 cycles. In contrast, conventional MPPT requires nearly 4 seconds (200cycles) respectively, for system restoration post-

Preprints.org (www.preprints.org) | NOT PEER-REVIEWED | Posted: 16 July 2024 doi:10.20944/preprints202407.1311.v1

fault occurrence. Fig--- depicts the DC link voltage between the PV system's back-to-back converters, revealing notable stability with the proposed technique Figure---. Convergence of the cost function is achieved in merely 9 iterations with the proposed IDGC. Optimal gain parameters yield reduced transients and an optimally responsive system. Overall, the proposed approach ensures efficient system stability and rapid response during fault scenarios, outperforming traditional methods in both damping capability and convergence speed. Further the results depicted in Figure 8, the direct axis voltage and current have been simulated. Three phase fault sustains for 1 second (4sec to 5 sec). In all the following simulation results the Conventional MPPT controller settles the system in 4second whereas the proposed IDGC technique achieves steady state condition in 1 second. Thus the proposed IDGC proves its superiority than the conventional MPPT controller in overshoot and settling time.

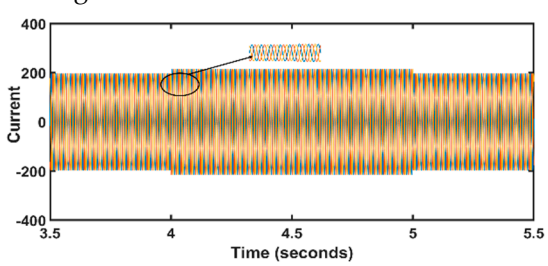

(a)

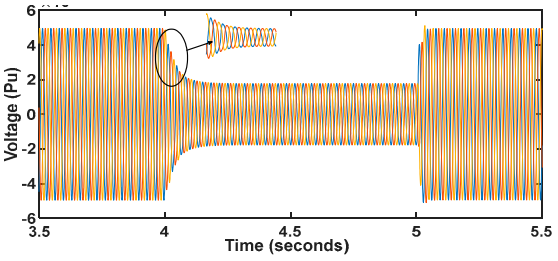

(b)

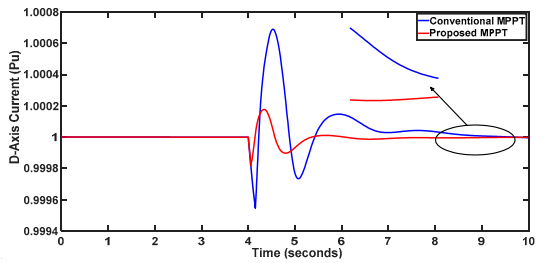

(c)

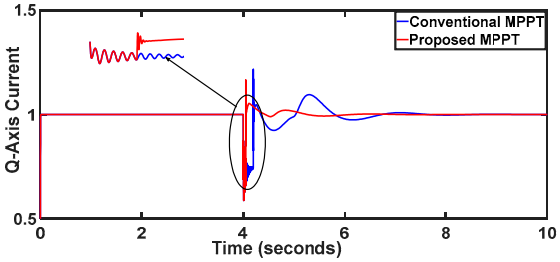

(d)

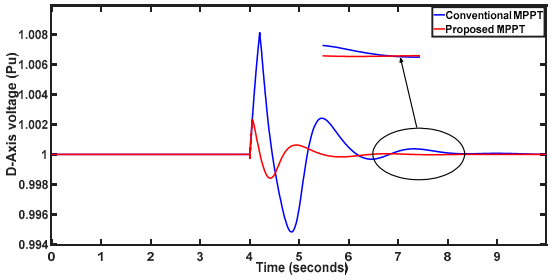

(e)

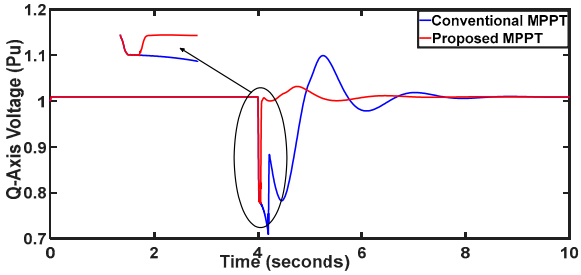

(f)

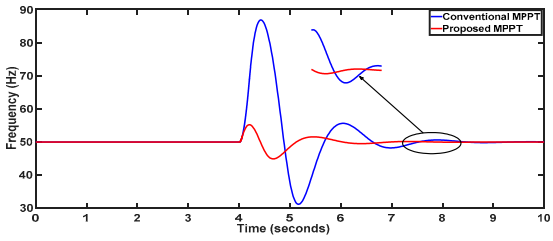

(g)

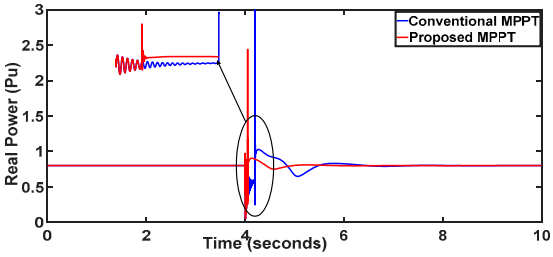

(h)

Preprints.org (www.preprints.org) | NOT PEER-REVIEWED | Posted: 16 July 2024 doi:10.20944/preprints202407.1311.v1

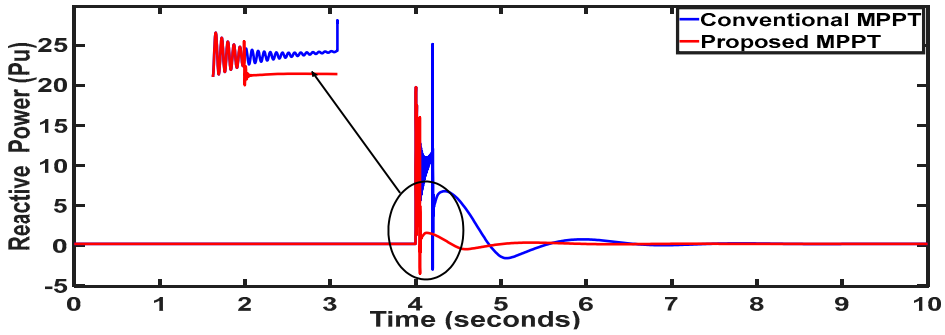

(i)

Figure 8. Performance of the proposed controller through (a) PCC current (b) PCC voltage (c) d-axis current (d) q-axis current (e) d-axis voltage (f) q-axis voltage (g) frequency (h) real power (i) reactive power.

Scenario-5: Islanding Operation

The Micro Grid behaviour is investigated with the proposed controller during islanding situation. At t = 1 s, intentional islanding is initiated via switch s1, as depicted in Fig.-9, focusing on the responses of PCC parameters. During islanding, the combined output from PV and battery adequately meets local load demand, ensuring stable bus-1 voltage through Distributed Generation (DG) supply amidst uncertainties. Notably, the proposed IDGC controller achieves system stabilization within a swift 0.5-second span, equivalent to 25 cycles (Figure 9a). In comparison, alternative methods require more cycles: the conventional MPPT controller-based Phase-Locked Loop (PLL) controller demands 100 cycles (2 s); the proposed controller exhibits heightened damping, resulting in diminished transient oscillations. Fig- Illustrates convergence graphs of optimization methods, showcasing the proposed controller's rapid convergence (merely 5 generations) with minimal error content. This underscores the efficacy of the proposed approach in swiftly stabilizing the system during intentional islanding, outperforming conventional methods in both convergence speed and transient response.

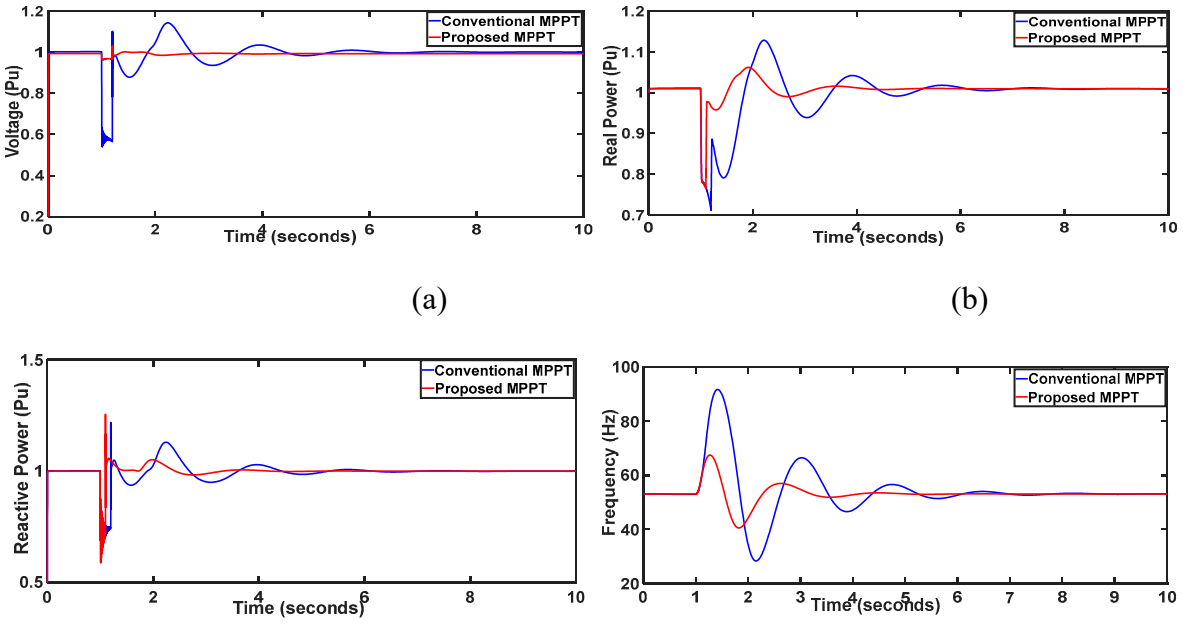

(a) (b)

(c) (d)

Preprints.org (www.preprints.org) | NOT PEER-REVIEWED | Posted: 16 July 2024 doi:10.20944/preprints202407.1311.v1

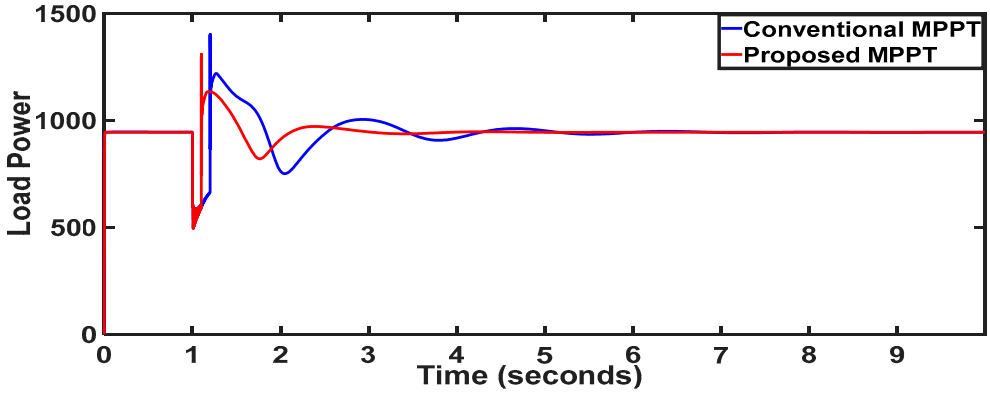

(e)

Figure 9. performance of the proposed controller through islanding condition (a) AC bus voltage (b) Real power (c) reactive power (d) frequency (e) load power.

Scenario-6: Load Change:

The performance evaluation extends to variations in load parameters, specifically at (PCC), where a 30% decrease occurs at t = 5 s followed by a 10% increase at t = 20 s, as depicted in Figure 10. The load current, as illustrated in Figure 10c,d, exhibits a corresponding decrease and subsequent increase in line with the load variation. Notably, despite these fluctuations, Figure 10a,b showcases the remarkable constancy of bus-1 voltage, indicative of effective controller operation, resulting in minimal deviation. Conversely, Figure 10e,f reveals the real and reactive power trend opposite to that of load current. The system's restoration time with the proposed IDGC controller stands at a mere 25 cycles (0.5 s), a notable improvement compared to the conventional technique requiring 50 cycles (1s). Furthermore, transient oscillations are notably subdued in the proposed method compared to the conventional techniques. Employing optimal IDGC method results in a system exhibiting superior transient profile and optimal functionality. The combination of reduced restoration time, minimized transient oscillations, and swift convergence of optimization underscores the effectiveness of the proposed approach in enhancing system stability and performance amidst load variations, offering significant advantages over conventional methods.

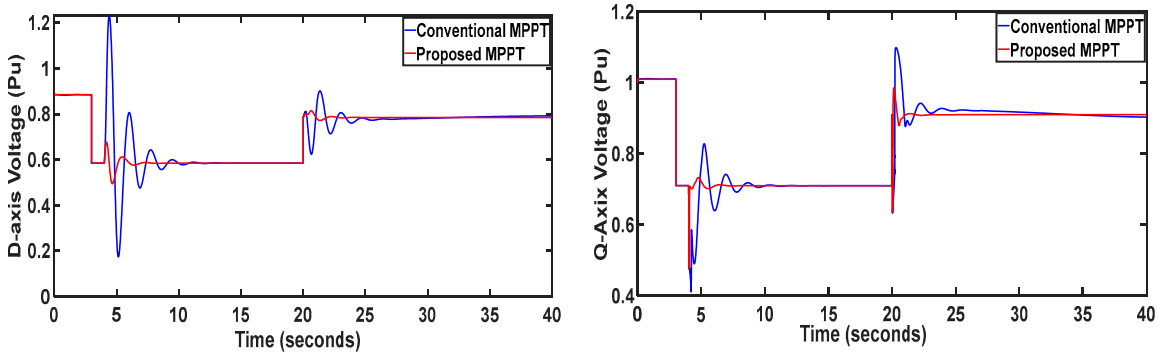

(a) (b)

Preprints.org (www.preprints.org) | NOT PEER-REVIEWED | Posted: 16 July 2024 doi:10.20944/preprints202407.1311.v1

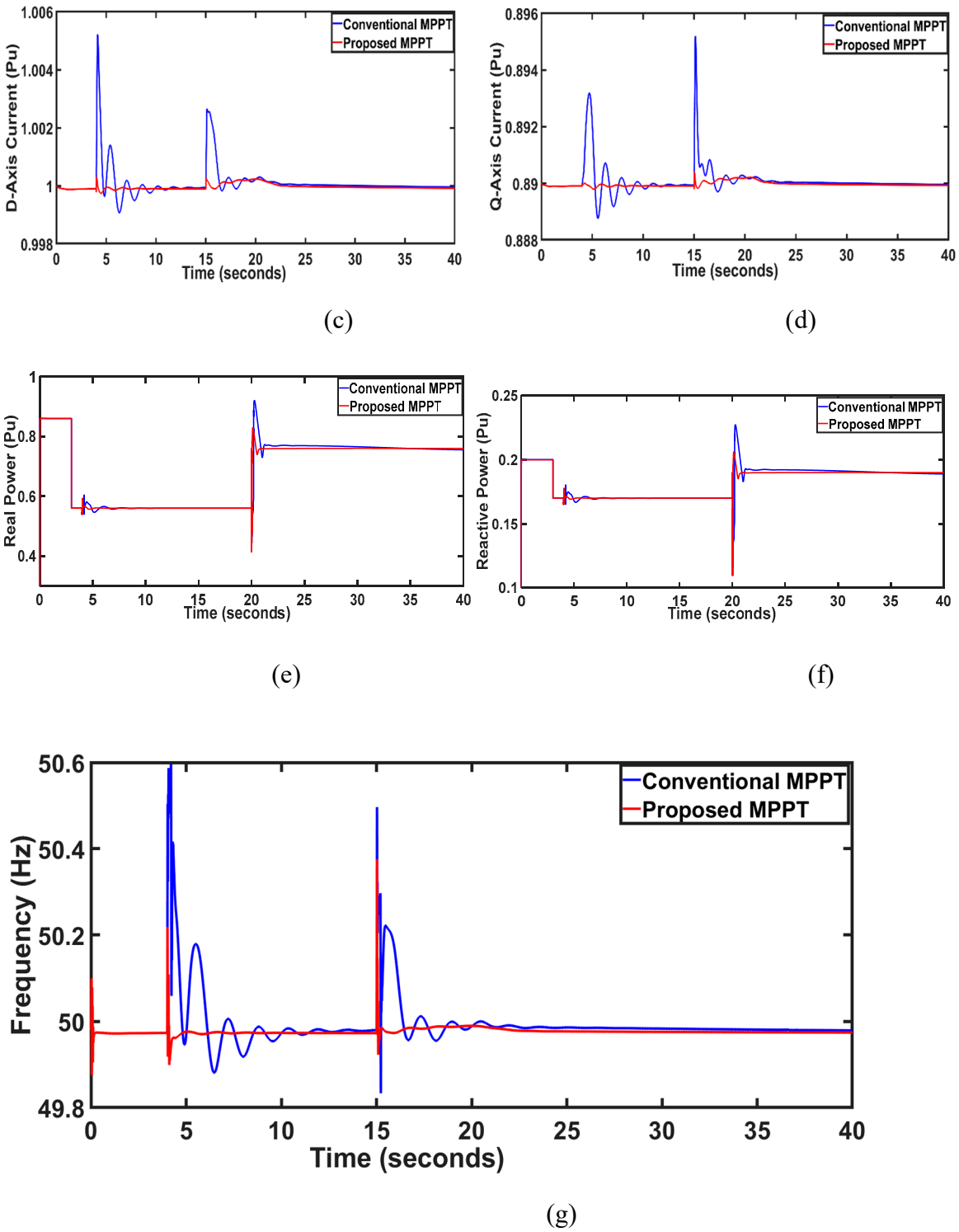

Figure 10. performance of the controller through load change (a) d-axis voltage (b) q-axis voltage (c) d-axis current (d) q-axis current (e) Real power (f) reactive power (g) Bus frequency.

Scenario-7: Hardware Validation

The validation of the performance of the proposed IDGC in a micro grid involves a Hardware-in-the-Loop (HIL) simulation. In this setup, the system, comprising a standard model with solar PV and battery energy storage (BES), is simulated using MATLAB Simulink. The PV-based DG is emulated using a PV emulator, specifically the Prototype solar plant, interfaced with Simulink as a 'Controlled Voltage Source'. Real-time data, including irradiation variation and partial shading, are captured through a dSPACE 1104 extension boards (ADC C5: DS1104 Master PPC library).

 doi:10.20944/preprints202407.1311.v1

The performance of the PV bus (PCC) is monitored by recording its RMS voltage & current, as depicted in Figure 11. To optimize the system's performance, controller gains are tuned using MATLAB script-based analysis and then implemented in the Simulink model. The irradiation profile for the PV is varied at specific time intervals, and data acquisition is facilitated by a digital-to-analogue converter (DS1104 C1 from DS1104 Master PPC library) connected to a TMS 320C6713 digital signal processor via Embedded USB JTAG. The collected data are visualized using a digital storage oscilloscope (DSO) (Tektronix TBS1022) through a Toshiba TLP 250 gate driver.

The conventional MPPT resulted in erroneous performance, manifesting in 150 cycles of dynamic oscillation. However, Figure 10, illustrates the improved performance of the controllers during solar irradiance variation when employing the proposed IDGC controller. Notably, compared to conventional PLL controllers, the proposed controller exhibits reduced oscillations and enhanced damping, leading to quicker system stabilization.

In summary, the HIL simulation validates the effectiveness of the proposed IDGC in mitigating uncertainties and stabilizing the micro grid system efficiently, as demonstrated through real-time emulation and performance analysis.

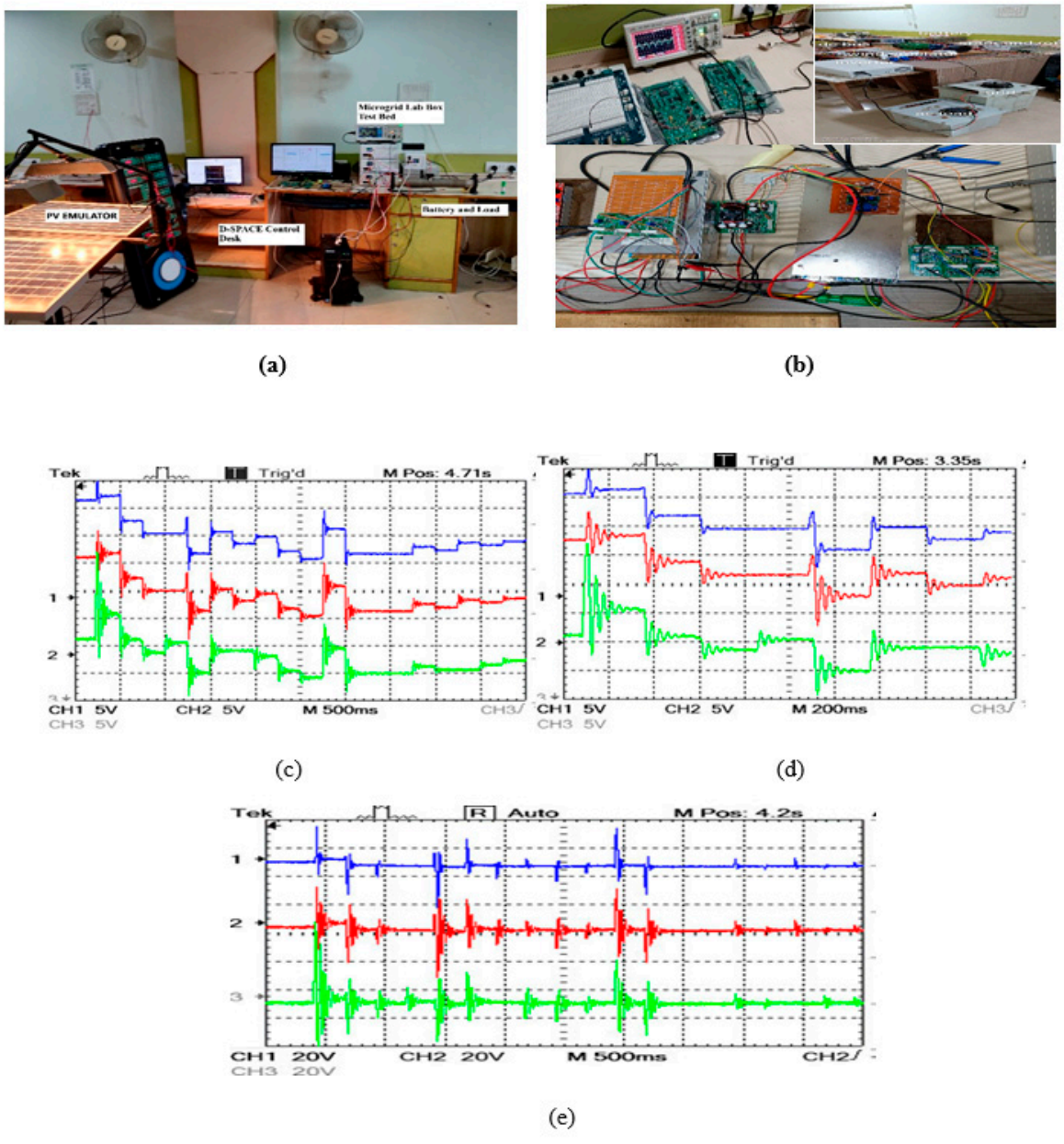

Figure 11. The performance of the proposed controller is validated through HIL in case of irradiance change (a) current in irradiance change (b) current in partial shading (c) voltage in irradiance change.

 doi:10.20944/preprints202407.1311.v1

5. Conclusion

A new IDGC, is suggested, utilizing an Extreme Learning Machine (ELM) for PV-based Distributed Generator (DG) operations. Compliant with ISA-95 and IEEE-1547 standards, it integrates MPPT and feedback control for standalone or grid-connected operation. The ELM-based IDGC aims to outperform traditional architectures by minimizing computation errors like e_{mppk} through reduced computational complexity. It replaces iterative ANN learning with (MPPI) technique, cutting computational delays. Regularization is achieved with a novel Ridge Regression estimated coefficient (RC), enhancing robustness against initial randomness. It is observed that the applied controller is more suitable and robust towards stability improvement in PV based MG. the proposed controller is tested in five case studies, like error minimization, irradiance change, partial shading, three phase fault, load change and islanding operations. The results are verified in MATLAB environment. It is observed that the proposed IDGC controller proved superior as compared to the conventional method. Finally the performance in irradiance change and partial shading is validated in Hardware in simulation (HIL) environment.

References

1. Saheb-Koussa D, Haddadi M, Belhamel M (2009) Economic and technical study of a hybrid system (wind–photovoltaic–diesel) forrural electrification in Algeria. Appl Energy 86(7–8):1024–1030
2. 2. Hu J, Shan Y, Yinliang X, Guerrero JM (2019) A coordinatedcontrol of hybrid ac/dc microgrids with PV-wind-battery under variable generation and load conditions. Int J Electr Power Energy Syst 104:583–592
3. M.A. Hannan , Shun Y. Tan , Ali Q. Al-Shetwi , Ker Pin Jern , R.A. Begum 'Optimized controller for renewable energy sources integration into micro grid: Functions, constraints and suggestions, Journal of Cleaner Production, Elsierver Volume 256, 20 May 2020, 120419
4. Swaminathan G, Ramesh V, Umashankar S, Sanjeevikumar P (2018) Investigations of microgrid stability and optimum power sharing using robust control of grid tie pv inverter. In: Advances in smart grid and renewable energy, Springer, Singapore, pp 379–387
5. Mohamed MA, Diab AAZ, Rezk H (2019) Partial shading mitigation of PV systems via different meta-heuristic techniques. Renew Energy 130:1159–1175
6. Mao M, Duan Q, Duan P, Bei H (2018) Comprehensive improvement of artificial fish swarm algorithm for global MPPT in PV system under partial shading conditions. Trans Inst Meas Control 40(7):2178–2199
7. Dhar S, Dash PK (2016) A new backstepping finite time sliding mode control of grid connected PV system using multivariable dynamic VSC model. Int J Electr Power Energy Syst 82:314–330
8. Patnaik RK, Dash PK, Mahapatra K (2016) Adaptive terminal sliding mode power control of DFIG based wind energy conversion system for stability enhancement. Int Trans Electr Energy Syst 26(4):750–782
9. Saffari M, de Gracia A, Fernández C, Belusko M, Boer D, Cabeza LF (2018) Optimized demand side management (DSM) of peak electricity demand by coupling low temperature thermal energy storage (TES) and solar PV. Appl Energy 211:604–616
10. Anand I, Senthilkumar S, Biswas D, Kaliamoorthy M (2018) Dynamic power management system employing a single-stage power converter for standalone solar PV applications. IEEE Trans Power Electron 33(12):10352–10362
11. Suresh M, Meenakumari R (2018) Optimal Planning of solar PV/WTG/DG/battery connected integrated renewable energy systems for residential applications using hybrid optimization. Int J Indu Eng 2(1):15–20
12. Mahdavi S, Hemmati R, Jirdehi MA (2018) Two-level planning for coordination of energy storage systems and wind-solar-diesel units in active distribution networks. Energy 151:954–965
13. Mahdi Mir, Mohammad Dayyani, Tole Sutikno, Morteza Mohammadi Zanjireh, Navid Razmjooy, ' Employing a Gaussian Particle Swarm Optimization method for tuning Multi Input Multi Output-fuzzy system as an integrated controller of a micro-grid with stability analysis, Computational intelligence willy, vol.36, No.1, 2020, PP.225-258.
14. Helmy M. El Zoghby a, Haitham S. Ramadan, 'Isolated microgrid stability reinforcement using optimally controlled STATCOM' Sustainable Energy Technologies and Assessments, Elsevier, Volume 50, March 2022, PP. 101883.
15. Moudud Ahmed , Lasantha Meegahapola , Arash Vahidnia, And Manoj Datta , 'Stability and Control Aspects of Microgrid Architectures, A Comprehensive Review' IEEE Access, 2020,Vol.08, PP. 144730

 doi:10.20944/preprints202407.1311.v1

16. P. K. Dash, Pravati Nayak, Prachitara Satapathy, Lokanath Tripathy, 'Optimal control of PV–WS battery-based microgrid using an adaptive water cycle technique' Electrical Engineering, 2020, Springer publications. PP. 2110-2114
17. Reddi Ganesh ,Tapas Kumar Saha , M.L.S. Sai Kumar,'Implementation of optimized extreme learning machine-based energy storage scheme for grid connected photovoltaic system' Journal of Energy Storage,Elsevier,2023 Vol.88, PP.1-13.
18. Amil Daraz, 'Optimized cascaded controller for frequency stabilization of marine micro grid system' Applied Energy, Elsevier, 2023, Vol.250,PP.1-18.
19. Najmeh Ghasemi , Mahmood Ghanbari , Reza Ebrahimi 'Intelligent and optimal energy management strategy to control the Micro-Grid voltage and frequency by considering the load dynamics and transient stability' International Journal of Electrical Power and Energy Systems, Elsevier, 2023,Vol.125, Vol.125, PP.1-13
20. Niranjan Nayak,Tanmoy Parida, Pravat Kumar Rout, Irani Majumder, And Sangram K. Routray, Dynamic stability improvement for VSC-HVDC-based inter connected power system using modified sliding mode controller', International Journal of Automation and Control, Inderscince, Vol.11, No2, PP.188-206.
21. Soliman MA, Hasanien HM, Azazi HZ, El-kholy EE, Mahmoud, SA (2018) Hybrid ANFIS-GA-based control scheme for performance enhancement of a grid-connected wind generator. IET Renew Power Gener 12(7):832–843.
22. Mohamed AAS, Berzoy A, Mohammed OA (2016) Design and hardware implementation of FL-MPPT control of PV systems based on GA and small-signal analysis. IEEE Trans Sustain Energy 8(1):279–290.
23. Dasu Butti , Siva Kumar Mangipudi, Srinivasa Rao Rayapudi , 'Design of robust modified power system stabilizer for dynamic stability improvement using Particle Swarm Optimization technique 'Ain Shams Engineering Journal Volume 10, Issue 4, December 2019, Pages 769-783
24. Real-time implementation of a novel MPPT control based on the improved PSO algorithm using an adaptive factor selection strategy for photovoltaic systems, ISA Transactions, Elsevier,Volume 146, March 2024, Pages 496-510
25. Mohammadi S, Soleymani S, Mozafari B (2014) Scenario-based stochastic operation management of microgrid including wind, photovoltaic, micro-turbine, fuel cell and energy storage devices. Int J Electr Power Energy Syst 54:525–535
26. Satapathy P, Dhar S, Dash PK (2017) Stability improvement of PV-BESS diesel generator-based microgrid with a new modified harmony search-based hybrid firefly algorithm. IET Renew Power Gen 11(5):566–577